Slewing Mirror Telescope optics for the early observation of UV/optical photons from Gamma-Ray Bursts

Jeong, S.; Nam, J. W.; Ahn, K. B.; Park, I. H.; Kim, S. W.; Lee, J.; Lim, H.; Brandt, Søren; Budtz-Jørgensen, Carl; Castro-Tirado, A. J.; Chen, P.; Cho, M. H.; Choi, J. N.; Grossan, B.; Huang, M. A.; Jung, A. ; Kim, J. E.; Kim, M. B.; Kim, Y. W.; Linder, E. V.; Min, K. W.; Na, G. W.; Panasyuk, M. I.; Ripa, J.; Reglero, V.; Smoot, G. F.; Suh, J. E.; Svertilov, S. ; Vedenkin, N. ; Yashin, I.

Published in:
Optics Express

Link to article, DOI:
10.1364/OE.21.002263

Publication date:
2013

Document Version
Publisher's PDF, also known as Version of record

Slewing Mirror Telescope optics for the early observation of UV/optical photons from Gamma-Ray Bursts

S. Jeong,[1] J. W. Nam, [2] K. B. Ahn,[3] I. H. Park,[5,*] S. W. Kim,[3,4] J. Lee,[5] H. Lim,[5] S. Brandt,[6] C. Budtz-Jørgensen,[6] A. J. Castro-Tirado,[7] P. Chen,[2] M. H. Cho,[1] J. N. Choi,[3] B. Grossan,[8] M. A. Huang,[9] A. Jung,[1] J. E. Kim,[1] M. B. Kim,[5] Y. W. Kim,[1] E. V. Linder,[8,11] K. W. Min,[10] G. W. Na,[1] M. I. Panasyuk,[11] J. Ripa,[5] V. Reglero,[12] G. F. Smoot,[8,11] J. E. Suh,[1] S. Svertilov,[11] N. Vedenkin,[11] and I. Yashin[11]

[1]Department of Physics, Ewha Womans University, 11-1 Daehyun-dong, Seoul 120-750, South Korea
[2]Department of Physics, National Taiwan University, 1 Roosevelt Road, Taipei, 106, Taiwan
[3]Department of Astronomy, Yonsei University, 134 Shinchon-dong, Seoul 120-749, South Korea
[4]Yonsei University Observatory, Yonsei University, 134 Shinchon-dong, Seoul 120-749, South Korea
[5]Department of Physics, Sungkyunkwan University, Seobu-ro, Jangangu, Suwonsi, Gyeongido, 440-746, South Korea
[6]Natinal Space Institute Astrophysics, Technical University of Denmark, 2800 Kgs. Lyngby, Denmark
[7]Instituto de Astrofisica de Andalucia (IAA-CSIC), P. O. Box 03004, E-18080 Granada, Spain
[8]University of California at Berkeley, Space Sciences Laboratory, 7 Gauss Way, Berkeley, CA 94720, USA
[9]Department of Energy Engineering, National United University, 1, Lienda, Miaoli, 36003, Taiwan
[10]Korea Advanced Institute of Science and Technology, 291 Daehak-ro, Yuseong-gu, Daejeon 305-701, South Korea
[11]Institute for the Early Universe, Ewha Womans University, 11-1 Daehyun-dong, Seoul 120-750, South Korea
[12]Skobeltsyn Institute of Nuclear Physics of Lomonosov, Moscow State University, Leninskie Gory, 119234, Russia
[13]Universidad de Valencia, GACE, Edif. de Centros de Investigacion, Burjassot, E-46100 Valencia, Spain
**ilpark@skku.edu*

Abstract: We report on design, manufacture, and testing of a Slewing Mirror Telescope (SMT), the first of its kind and a part of Ultra-Fast Flash Observatory-pathfinder (UFFO-p) for space-based prompt measurement of early UV/optical light curves from Gamma-Ray Bursts (GRBs). Using a fast slewing mirror of 150 mm diameter mounted on a 2 axis gimbal stage, SMT can deliver the images of GRB optical counterparts to the intensified CCD detector within 1.5~1.8 s over ± 35 degrees in the slewing field of view. Its Ritchey-Chrétien telescope of 100 mm diameter provides a 17 × 17 arcmin^2 instantaneous field of view. Technical details of design, construction, the laboratory performance tests in space environments for this unique SMT are described in conjunction with the plan for in-orbit operation onboard the *Lomonosov* satellite in 2013.

OCIS codes: (110.0110) Imaging systems; (220.0220) Optical design and fabrication.

References and links

1. C. Meegan, G. Fishman, R. Wilson, J. Horack, M. Brock, W. Paciesas, G. Pendleton, and C. Kouveliotou, "Spatial distribution of γ-ray bursts observed by BATSE," Nature **355**(6356), 143–145 (1992).
2. R. Klebesadel, I. Strong, and R. Olson, "Observations of gamma-ray bursts of cosmic origin," ApJ **182**, L85–L88 (1973).
3. E. Costa, F. Frontera, J. Heise, M. Feroci, J. Zand, F. Fiore, M. Cinti, D. Fiume, G. Zavattini, R. Jager, A. Parmar, A. Owens, S. Molendi, G. Cusumano, M. Maccarone, S. Giarrusso, A. Coletta, L. Antonelli, P. Giommi, J. Muller, L. Piro, and R. Butler, "Discovery of an x-ray afterglow associated with the γ-ray bursts of 28 February 1997," Nature **387**, 783–785 (1997).
4. N. Gehrels, G. Chincarini, P. Giommi, K. Mason, J. Nousek, A. Wells, N. White, S. Barthelmy, D. Burrows, L. Cominsky, K. Hurley, F. Marshall, P. Mészáros, P. Roming, L. Angelini, L. Barbier, T. Belloni, S. Campana, P. Caraveo, M. Chester, O. Citterio, T. Cline, M. Cropper, J. Cummings, A. Dean, E. Feigelson, E. Fenimore, D. Frail, A. Fruchter, G. Garmire, K. Gendreau, G. Ghisellini, J. Greiner, J. Hill, S. Hunsberger, H. Krimm, S. Julkarni, P. Kumar, F. Lebrun, N. Lloyd-Ronning, C. Markwardt, B. Mattson, R. Mushotzky, J. Norris, J. Osborne, B. Paczynski, D. Palmer, H. Park, A. Parsons, J. Paul, M. Rees, C. Reynolds, J. Rhoads, T. Sasseen, B. Schaefer, A. Short, A. Smale, I. Smith, L. Stella, G. Tagliaferri, T. Takahashi, M. Tashiro, L. Townsley, J.

#179532 - $15.00 USD Received 8 Nov 2012; revised 27 Dec 2012; accepted 2 Jan 2013; published 23 Jan 2013

Tueller, M. Turner, M. Vietri, W. Voges, M. Ward, R. Willingale, F. Zerbi, and W. Zhang, "The *Swift* Gamma-Ray Burst mission," ApJ **611**(2), 1005–1020 (2004).
5. A. Castro-Tirado, J. Soldán, M. Bernas, P. Páta, T. Rezek, R. Hudec, T. Sanguino, B. Morena, J. Berná, J. Rodríguez, A. Peña, J. Gorosabel, J. Máshesse, and A. Giménez, "The Burst Observer and Optical Transient Exploring System (BOOTES)," Astron. Astrophys. Suppl. Ser. **138**(3), 583–585 (1999).
6. C. Akerlof, R. Kehoe, T. Mckay, E. Rykoff, D. Smith, D. Casperson, K. Mcgowan, W. Vestrand, P. Wozniak, J. Wren, M. Ashley, M. Phillips, S. Marshall, H. Epps, and J. Schier, "The ROTSE-III robotic telescope system," Publ. Astron. Soc. Pac. **115**(803), 132–140 (2003).
7. F. Zerbi, G. Chincarini, G. Ghisellini, M. Rodonó, G. Tosti, L. Antonelli, P. Conconi, S. Covino, G. Cutispoto, E. Molinari, L. Nicastro, E. Palazzi, C. Akerlof, L. Burderi, S. Campana, G. Crimi, J. Danzinger, A. Paola, A. Fernandez-soto, F. Fiore, F. Frontera, D. Fugazza, G. Gentile, P. Goldoni, G. Israel, B. Jordan, D. Lorenzetti, B. Breen, E. Martinetti, R. Mazzoleni, N. Masetti, S. Messina, E. Meurs, A. Monfardini, G. Nucciarelli, M. Orlandini, J. Paul, E. Pian, P. Saracco, S. Sardone, L. Stella, L. Tagliaferri, M. Tavani, V. Testa, and F. Vitali, "The REM telescope: detecting the near infrared counterparts of Gamma-Ray Bursts and the prompt behavior of their optical continuum," Astron. Nachr. **322**(5-6), 275–285 (2001).
8. A. Klotz, F. Vachier, and M. Böer, "TAROT: robotic observatories for gamma-ray bursts and other sources," Astron. Nachr. **329**(3), 275–277 (2008).
9. W. T. Vestrand, P. R. Wozniak, J. A. Wren, E. E. Fenimore, T. Sakamoto, R. R. White, D. Casperson, H. Davis, S. Evans, M. Galassi, K. E. McGowan, J. A. Schier, J. W. Asa, S. D. Barthelmy, J. R. Cummings, N. Gehrels, D. Hullinger, H. A. Krimm, C. B. Markwardt, K. McLean, D. Palmer, A. Parsons, and J. Tueller, "A link between prompt optical and prompt gamma-ray emission in Gamma-Ray Bursts," Nature **435**(7039), 178–180 (2005).
10. J. Racusin, S. Karpov, M. Sokolowski, J. Granot, X. Wu, V. Palshin, S. Covino, A. Horst, S. Oates, P. Schady, R. Smith, J. Cummings, R. Starling, L. Piotrowski, B. Zhang, P. Evans, S. Holland, K. Malek, M. Page, L. Vetere, R. Margutti, C. Guidorzi, A. Kamble, P. Curran, A. Beardmore, C. Kouveliotou, L. Mankiewicz, A. Melandri, P. Obrien, K. Page, T. Piran, N. Tanvir, G. Wrochna, R. Aptekar, C. Bartolini, S. Barthelmy, G. Beskin, S. Bondar, S. Campana, A. Cucchiara, M. Cwiok, P. D'Avanzo, V. D'Elia, M. Della Valle, W. Dominik, A. Falcone, F. Fiore, D. Fox, D. Frederiks, A. Fruchter, D. Fugazza, M. Garrett, N. Gehrels, S. Golenetskii, A. Gomboc, G. Greco, A. Guarnieri, S. Immler, G. Kasprowicz, A. Levan, E. Mazets, E. Molinari, A. Moretti, K. Nawrocki, P. Oleynik, J. Osborne, C. Pagani, Z. Paragi, M. Perri, A. Piccioni, E. Ramirez-Ruiz, P. Roming, I. Steele, R. Strom, V. Testa, G. Tosti, M. Ulanov, K. Wiersema, R. Wijers, A. Zarnecki, F. Zerbi, P. Mészáros, G. Chincarini, and D. Burrows, "GRB 080319B: A naked-eye stellar blast from the distant universe," Nature **455**, 183–188 (2008).
11. I. Park, S. Ahmad, P. Barrillon, C. Budtz-Jørgensen, A. Castro-Tirado, P. Chen, Y. Choi, P. Connell, S. Dagoret-Campagne, C. Eyles, B. Grossan, M. Huang, A. Jung, S. Jeong, J. Kim, M. Kim, S. Kim, Y. Kim, A. Krasnov, J. Lee, H. Lim, E. Linder, T. Liu, N. Lund, K. Min, G. Na, J. Nam, M. Panasyuk, J. Ripa, V. Reglero, J. Rodrigo, G. Smoot, J. Suh, S. Svertilov, N. Vedenkin, M. Wang, and I. Yashin, "Ultra-Fast Flash Observatory (UFFO) for observation of early photons from Gamma-Ray Bursts," accepted to New J. of Physics (2013).
12. I. Park, "MEMS based space telescope for extreme energy cosmic ray experiments," Nucl. Phys. B **134**(Suppl.), 196–201 (2004).
13. J. Lee, J. Kim, G. Na, J. Jeon, S. Jeong, A. Jung, H. Lee, J. Nam, J. Suh, G. Garipov, P. Klimov, B. Khrenov, M. Panasyuk, N. Vedenkin, and I. Park, "A new type of space telescope for observation of extreme lightning phenomena in the upper atmosphere," IEEE Trans. Geosci. Rem. Sens. **50**(10), 3941–3949 (2012).
14. J. H. Park, G. K. Garipov, J. A. Jeon, B. A. Khrenov, J. E. Kim, M. Kim, Y. K. Kim, C. H. Lee, J. Lee, G. W. Na, S. Nam, I. H. Park, and Y. S. Park, "Obscura telescope with a MEMS micromirror array for space observation of transient luminous phenomena or fast-moving objects," Opt. Express **16**(25), 20249–20257 (2008).
15. B. W. Yoo, J. H. Park, I. H. Park, J. Lee, M. Kim, J. Y. Jin, J. A. Jeon, S. W. Kim, and Y. K. Kim, "MEMS micromirror characterization in space environments," Opt. Express **17**(5), 3370–3380 (2009).
16. K. Chase and A. Parkinson, "A survey of research in the application of tolerance analysis to the design of mechanical assemblies," Res. Eng. Des. **3**(1), 23–37 (1991).
17. The Soyuz company, *Russia's Soyuz Launch Vehicle User's Manual* (Starsem, 2001), Chap. 3.
18. Schott, ZERODUR® zero expansion glass ceramic (Germany, 2011).
19. ZEMAX development corporation, *ZEMAX® Optical Design Program User's Guide* (2005).
20. J. Y. Wang and D. E. Silva, "Wave-front interpretation with Zernike polynomials," Appl. Opt. **19**(9), 1510–1518 (1980).
21. P. Yoder, *Opto-Mechanical Systems Design* (Marcel Dekker Incorporated, 1993).
22. P. Bely, *The Design and Construction of Large Optical Telescopes* (Springer, 2003).
23. J. Cheng, *The Principles of Astronomical Telescope Design* (Springer, 2009).

1. Introduction

Over the last decades, several studies have improved our understanding of Gamma-Ray Burst (GRB) physics [1–4]. In particular, *Swift* observatory has localized accurately the locations of UV/optical counterparts of hundreds of GRBs in typically 100 s after the gamma ray trigger, since its commencement of in-orbit measurement in 2004. With GRBs Coordinate Network (GCN) circulars via SMSs and e-mails, ground robotic telescopes, such as ROTSE-III, REM,

#179532 - $15.00 USD Received 8 Nov 2012; revised 27 Dec 2012; accepted 2 Jan 2013; published 23 Jan 2013

TAROT and BOOTES [5–8] have observed optical, infrared and radio counterparts of GRBs. However, due to the inherent slow response time for slewing the whole satellite and/or ground telescopes, only a few early UV/optical light curve measurements are available to the world wide academic communities as of today [9,10].

This gives rise to an urgent necessity for a new and faster instrument capable of GRB UV/optical counterpart measurement within a few seconds after the gamma ray trigger from GRBs. The Ultra-Fast Flash Observatory (UFFO) has been proposed to measure on such time scales [11,12] by utilizing a fast slewing mirror [12–15], as shown in Fig. 1.

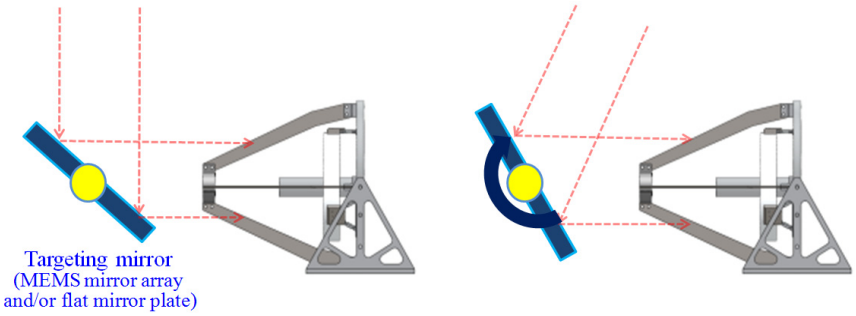

Fig. 1. Concept of SMT [12].

As the first one of its kind, the UFFO-pathfinder instrument has been developed as one of science payloads onboard the *Lomonosov* satellite that is scheduled to be launched in 2013. The UFFO-pathfinder consists of two instruments as in Fig. 2: the UFFO Burst Alert and Trigger Telescope (UBAT) and SMT. UBAT is the X-ray trigger telescope with a coded mask and YSOs (Yttrium Orthosilicate) + MAPMTs (Multianode photomultiplier) array detector plane.

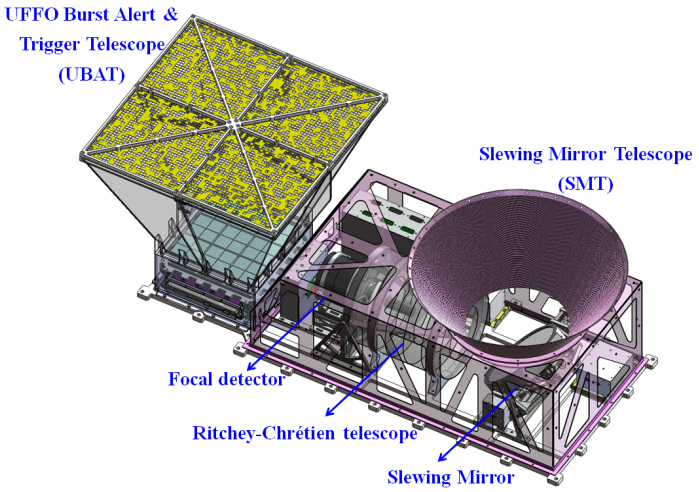

Fig. 2. Rendering view of UFFO-pathfinder.

When UBAT provides a trigger signal and approximate coordinates of a GRB to SMT, the SMT slewing mirror rotates quickly to the target coordinate and brings images of the UV/optical counter parts of GRB into the instrument FOV (Field of view) much faster than the ~60 s of the *Swift* instrument. Once the image has been delivered within the SMT FOV, it is acquired within 1 s in settling and readout time. To realize such a measurement concept, SMT consists of a slewing mirror mounted on a 2 axis gimbal stage, a Ritchey-Chrétien telescope (RC telescope), a focal plane Intensified Charge-Coupled Device (ICCD) detector and associated readout electronics.

#179532 - $15.00 USD Received 8 Nov 2012; revised 27 Dec 2012; accepted 2 Jan 2013; published 23 Jan 2013

Excluding the focal plane detector and its associated electronics, this paper describes the technical details of SMT, focusing on the design, manufacture, integration and test (I & T) including space environment tests and the laboratory scale end-to-end validation tests before the scheduled launch. First, the SMT design, fabrication, assembly and initial test results are presented in section 2. In section 3, the space environment tests of the integrated SMT are summarized together with the results. The laboratory scale end-to-end performance tests and their results are reported in section 4. In section 5 discusses the development and prospect of large SMT for future application, before concluding remarks in section 6.

2. SMT RC telescope and slewing mirror assembly

2.1. RC telescope design and construction

2.1.1. RC telescope optical design

Table 1. Requirements for SMT optics

SMT optics	Slewing mirror and RC telescope
Aperture size	10 cm
Slewing coverage	70 × 70 arcdeg^2
Slewing speed	> 35 degrees / s
Detector FOV	17 × 17 arcmin^2
Angular resolution	4 arcsec
Advanced resolution	0.5 arcsec (after centroiding)
Modulation Transfer Function	> 0.4 at 22.52 mm^{-1}
Sensitive wavelength	200~650 nm
Mass	3 kg
Volume	600 (l) × 320 (w) × 200 (h) mm^3

The SMT optical system consists of a slewing mirror and a RC telescope and has its system requirements summarized in Table 1. The RC telescope uses a primary mirror (M1) of 100 mm in diameter and −1.01 in conic coefficient and a secondary mirror (M2) of 20 mm in diameter and −1.83 in conic coefficient, located about 130 mm away. The telescope has 1.14 m effective focal length and fits within 200 mm in UFFO-pathfinder (Fig. 3). It is intended to produce 17 × 17 arcmin^2 in instantaneous FOV (IFOV) on the detector. The design results in an almost diffraction limited performance, with a Modulation Transfer Function (MTF) of 0.77 at 22.52 mm^{-1} Nyquist frequency and an on-axis RMS spot radius of 2.48 μm. Its spot diagrams over the SMT FOV are well within the Airy disk of 400 nm in diameter. The optics design satisfies all the RC telescope performance requirements as listed in Table 1.

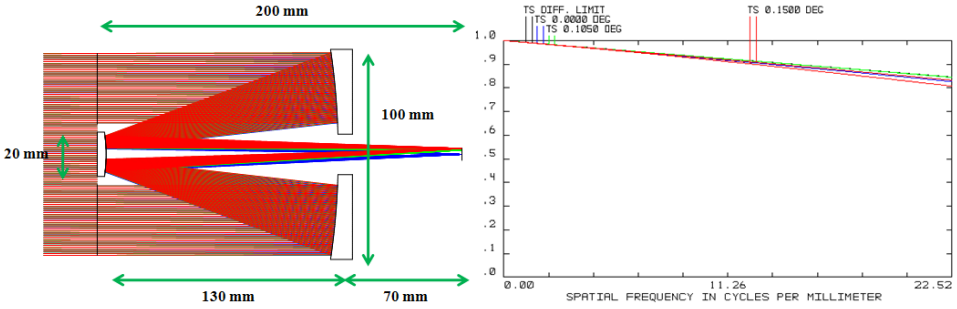

Fig. 3. 2D ray tracing of RC telescope (left) and the MTF performance (right).

#179532 - $15.00 USD Received 8 Nov 2012; revised 27 Dec 2012; accepted 2 Jan 2013; published 23 Jan 2013

2.1.2. Opto-mechanical structures of RC telescope

The telescope primary mirror (M1) is mounted to the M1 support plate via 3 bi-pod flexures as shown in Fig. 4. The telescope secondary mirror (M2) cell is then mounted to the M1 support plate by 4 spider arms. For all flexures and 4 spider arms, Invar36 is used to minimize thermal variation of distance between M1 and M2. To minimize the stress on M1 caused by a mismatch in thermal expansion coefficient (CTE) between the Invar flexure and the aluminum support structure, the bipod legs are designed to 12 mm long, 2 mm wide, and 1.5 mm thick. The M2 cell has an invar spider core with 3 flexure blades of 3.5 mm long, 3 mm wide and 0.3 mm thick. This provides the minimum obscuration ratio, down to 12.5%. Using tetrahedron curvature based mesh elements, Finite Element Analysis (FEA) was performed for the RC opto-mechanical structure under thermal loading for temperature variations over 30 °C range.

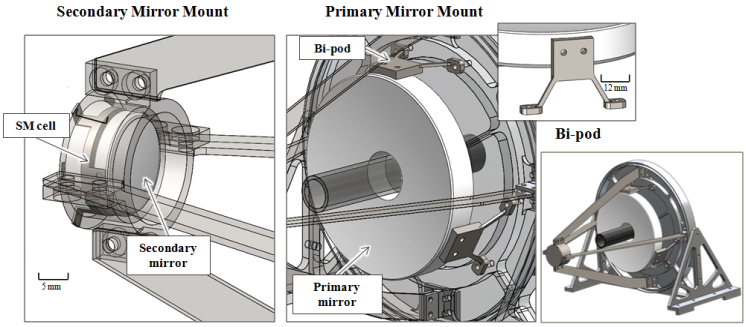

Fig. 4. Design of PM bipod and SM flexure in RC opto-mechanical design.

Table 2. Static thermal analysis result for temperature variations (ΔT) of 30°C in RC telescope

SM parameter	Unit	Tolerance	Analysis result (Abs.)
X decenter	mm	$\pm 2.00 \times 10^{-2}$	2.58×10^{-4}
Y decenter	mm	$\pm 2.00 \times 10^{-2}$	7.26×10^{-3}
X tilt	degrees	$\pm 5.00 \times 10^{-2}$	1.19×10^{-3}
Y tilt	degrees	$\pm 5.00 \times 10^{-2}$	5.70×10^{-4}
Z defocus	mm	$\pm 5.00 \times 10^{-3}$	4.21×10^{-6}
RMS WFE	waves	1/20	1/40

One of the base-plate edges is constrained in 6 degrees of freedom (DOF) and three surfaces that share the edge are constrained in sliding contact from each other, while allowing for expansion and contraction in either direction. The thermal analysis results listed in Table 2 show that the alignment variation of the RC telescope would be smaller than the tolerance and hence the optical performance would survive in the thermal environment in orbit. The expected Root Mean Square (RMS) Wave Front Error (WFE) is 1/40 waves, which is well below the WFE tolerance.

#179532 - $15.00 USD Received 8 Nov 2012; revised 27 Dec 2012; accepted 2 Jan 2013; published 23 Jan 2013

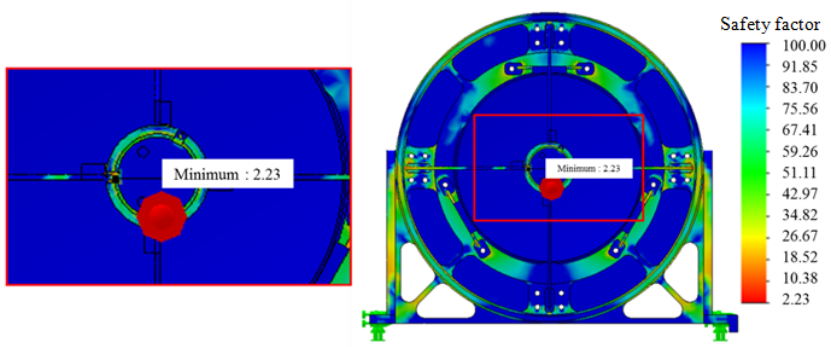

Fig. 5. 50 g static load analysis view in RC telescope: minimum safety factor is 2.23 in launch direction.

While constraining 8 fasteners of the joints in 6 DOF between the base-plate and the RC telescope, the static and modal analysis were performed to understand the launch survivability of the design under 50 g loading condition. As Fig. 5 shows, the results give 2.23 for the minimum safety factor, which denotes the ratio of maximum stress on the component to the ultimate strength that the component can receive before breakage, along the launch direction. The first resonance mode appears at 135 Hz, which is well above the typical payload frequency requirement of 50 Hz [17]. The analysis results demonstrate that the RC telescope would survive under the launch stress.

2.1.3. Fabrication and integration of RC telescope

All mirrors are made of *Zerodur* [18] substrates, coated with SiO_2 + Al for average reflectivity (R_{avg}) $\gtrsim$ 85% as shown in Fig. 6. The manufactured mirror characteristics are listed in Table 3. The opto-mechanical components were manufactured to meet the fabrication tolerance. M1 and M2 are bonded to the bi-pod flexures and its cell respectively, using EC2216B/A epoxy. The final alignment of the RC telescopes was measured with a WYCO RTI6100 phase shifting interferometer as shown in Fig. 7. The resulting RMS system WFE was found to be 22.3 nm for 633 nm in wavelength (Fig. 7), which is well within the WFE requirement of < 0.15 waves. This system performance demonstrates that the SMT fabrication and integration are successfully controlled within the tolerance.

Table 3. SMT mirror characteristics for both designed and manufactured mirrors

	Primary mirror		Secondary Mirror		Slewing Mirror	
	Design	Manufac.	Design	Manufac.	Design	Manufac.
Radius curvature (mm)	315.0 ± 0.3	315.3	−63.8 ± 0.3	−63.80	Infinity	Infinity
Conic constant	−1.01 ± 0.01	−1.02	−1.83 ± 0.01	−1.83	-	-
RMS surface wavefront error (waves)	1/30	1/44	1/30	1/69	1/30	1/43

#179532 - $15.00 USD Received 8 Nov 2012; revised 27 Dec 2012; accepted 2 Jan 2013; published 23 Jan 2013

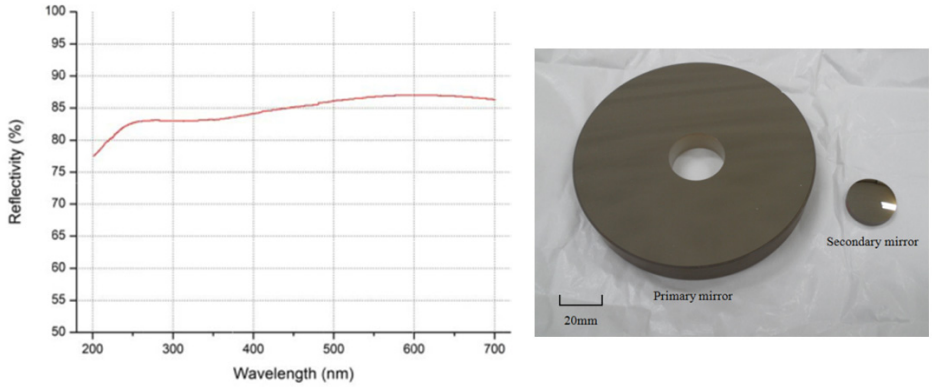

Fig. 6. Measured mirror reflectivity as function of wavelength, and the manufactured mirrors.

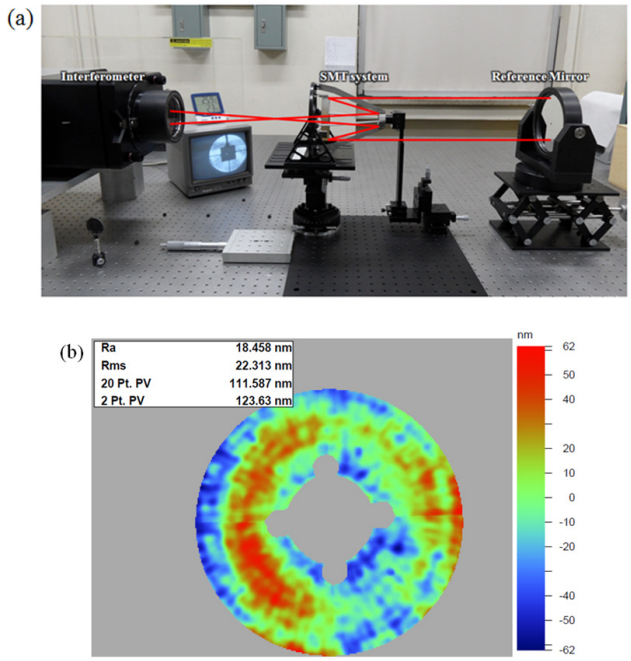

Fig. 7. (a) Experimental setup for RC telescope alignment and (b) measured system RMS WFE.

2.1.4. Static load test in laboratory

The static load test was performed to evaluate the launch survivability of the RC telescope over 0~29.4 N in load condition, simulating 0~60 g in acceleration applied to the M2 assembly. As shown in Fig. 8, the load was increased and decreased, and the M2 assembly coordinate was measured with a micrometer. The results show a typical but small hysteresis characteristic of up to about 3 μm that is still within the M2 decenter tolerance. And the hysteresis characteristic becomes negligible when the applied load is reduced back to 0 N, demonstrating that the RC telescope would survive under the launch stress.

#179532 - $15.00 USD Received 8 Nov 2012; revised 27 Dec 2012; accepted 2 Jan 2013; published 23 Jan 2013

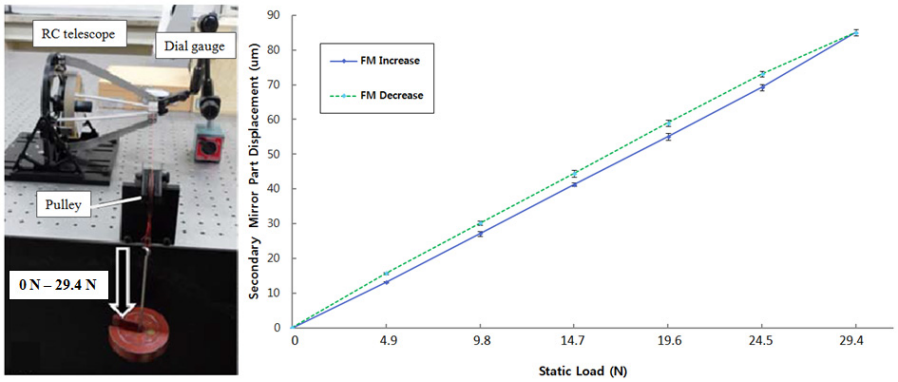

Fig. 8. The static load test to evaluate the launch survivability of the RC Telescope.

2.2. Slewing mirror assembly

2.2.1. Slewing mirror design

The flat slewing mirror is mounted onto the slewing mirror stage and redirects the incident light to the RC telescope as shown in Fig. 2. Given the limited mass and volume budget, the slewing mirror is designed to 15 cm in diameter and illuminates the full aperture of the RC telescope on-axis. For an off-axis incoming beam of light, it feeds only about 80% of the RC telescope aperture area. The honeycomb mirror design achieved 57% mass reduction; the final mirror was only 482 g yet sufficiently stiff for our purposes.

2.2.2. Slewing mirror stage design

The slewing mirror stage has an aluminum support ring and RTV566 pads are inserted between the ring and mirror around its peripheral, front and back surfaces. A two axes gimbal stage with stepper motors and rotary encoders is used, and its inner axis (A) bracket holds the mirror support ring while being mounted to the outer axis (B) bracket. The B axis stepping motor is designed to locate the slewing mirror surface so that its rotation axis is aligned with the RC telescope optical axis. The stepping motors have 200 steps / rev, providing ~4 arcsec in rotation step size with 100:1 harmonic drive gears. Using the closed-loop control in conjunction with the rotary encoders, the rotation angle can be controlled precisely to 2 arcmin in accuracy. The opto-mechanical design of the slewing mirror system is presented in Fig. 9.

Using tetrahedron type curvature based element mesh, the static FE thermal analysis over 30 degrees in thermal change was performed with the slewing mirror center as the constraint point, yet allowing for a free thermal expansion of the aluminum ring cover and of the slewing mirror. The resulting thermal deformation of the surface would be around 26 nm in low spatial frequency and 2 nm in high spatial frequency as shown in Table 4, again satisfying the requirements [19–21].

Table 4. Static thermal analysis result for ΔT = 30°C of slewing mirror and opto-mechanical design

Parameter	Requirement on surface irregularity (nm)	Analysis result (Abs., nm)
Irregularity of low spatial frequencies	40	26
Irregularity of high spatial frequencies	20	2

#179532 - $15.00 USD Received 8 Nov 2012; revised 27 Dec 2012; accepted 2 Jan 2013; published 23 Jan 2013

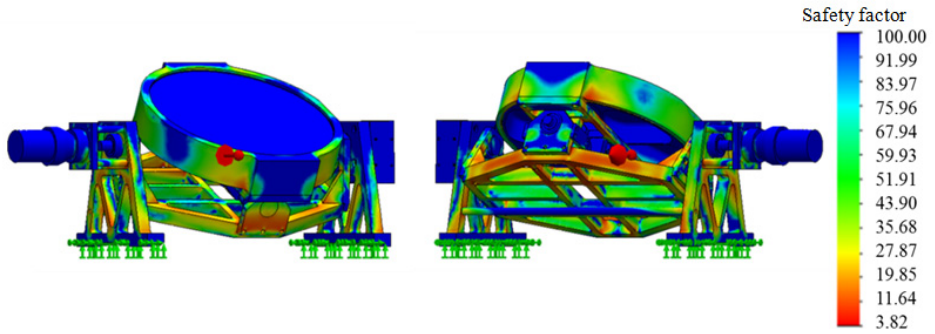

Fig. 9. Example of the safety factor distribution over the slewing mirror system under 50 g static load analysis.

With the 6 DOF constraints on 8 joint fasteners between the base-plate and the slewing mirror, modal and static FE analysis were performed. The result is 108.7 Hz for the first resonance frequency, well above the typical frequency requirement of 50 Hz [17]. The static load analysis showed a safety factor of 3.82 under 50 g loads along the launch axis as shown in Fig. 9, and 2.84 in minimum safety factor along the other axes.

2.2.3. Fabrication and assembly of slewing mirror system

The *Zerodur* light-weighted slewing mirror weighs 482 g to satisfy the mass budget < 0.6 kg. The slewing mirror surface as fabricated fulfills the RMS surface WFE target as presented in Table 3. The slewing mirror is also coated with SiO_2 + Al and found to have $R_{avg} \gtrsim 85\%$, and can be rotated from + 22.25° to –21.47° in inner A axis and from + 66.26° to –2.25° in outer B axis on average (+ is in direction of arrow in Fig. 10). This allows for the full ± 35 degrees in sky coverage. The total mass of the slewing mirror assembly is measured as about 1.85 kg, satisfying the mass requirement of < 2 kg.

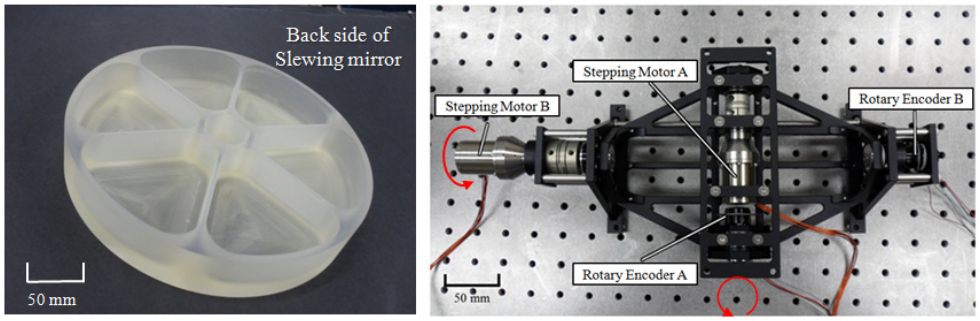

Fig. 10. The manufactured light-weighted slewing mirror (before SiO_2 + Al coating) and gimbal stage.

2.2.4 Slewing mirror performances: speed, pointing accuracy and settling time

The slewing mirror was moved from its initial on-axis position to ± 35 degrees at ~10 degrees intervals on each axis. The duration of the motor clock was checked to find the slewing speed. The angular speed is around 1.5 s on average over ± 35 degrees in sky coverage for each axis and its absolute positioning accuracy is around 2.56 arcmin.

#179532 - $15.00 USD Received 8 Nov 2012; revised 27 Dec 2012; accepted 2 Jan 2013; published 23 Jan 2013

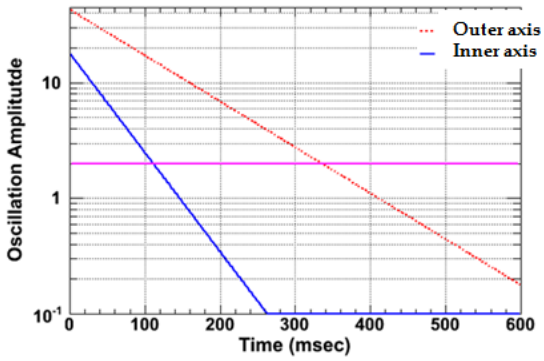

Fig. 11. Measured oscillation amplitude in unit of arcsec versus time. The settling time is defined as the time taken for an oscillation less than one half of pixel size, i.e. 2 arcsec as shown by the pink horizontal line.

To measure the settling time of the slewing mirror, we measured the position of a laser reflected by the mirror. Vibration settles to < 4 arcsec (the pixel size of our detector) in 110 ms for the outer (B) and 340 ms for the inner (A) axes respectively, as shown in Fig. 11. Currently, we find the time for moving plus settling to be ~1.6 s and 1.8 s over ± 35 degrees FOV for the inner and outer axes, respectively. We intend to improve this to 1 s for 35 degrees slews by an optimization of the motor control algorithm before launch.

3. Space environment tests for SMT optics

3.1. Space environment tests

The *Lomonosov* satellite will be orbiting around the Earth once every 96 min at 509 km in altitude. Therefore, the thermal loading profile to the satellite would have 48 min for heating, followed by another 48 min for cooling over the temperature range of –30°C to 40 °C (i.e. 70 °C/ hour in maximum temperature slope). With these conditions in mind, it was exposed to four temperature cycles repeatedly for about 48 hours. The test was performed at a high vacuum level of 10^{-6} mbar. Thermocouples were attached to the 18 designated locations on the RC telescope and slewing mirror assembly including the reverse of M1, M2 and the slewing mirror. Figure 12 shows examples of the thermocouples' locations on the SMT optics, and typical examples of thermocouple response to the thermal loading are shown in Fig. 13.

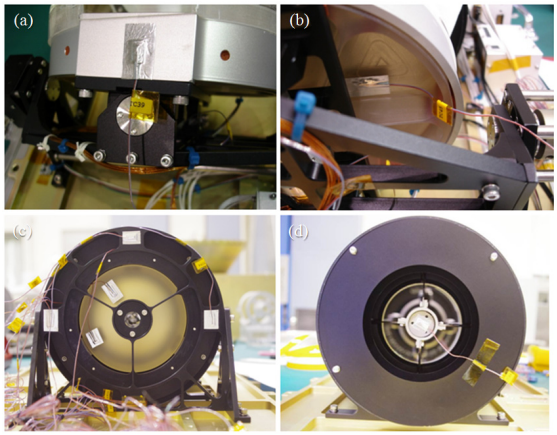

Fig. 12. Thermocouple locations on the (a) Al ring structure of the slewing mirror, (b) reverse of the slewing mirror, (c) RC telescope, and (d) SM cell.

#179532 - $15.00 USD Received 8 Nov 2012; revised 27 Dec 2012; accepted 2 Jan 2013; published 23 Jan 2013

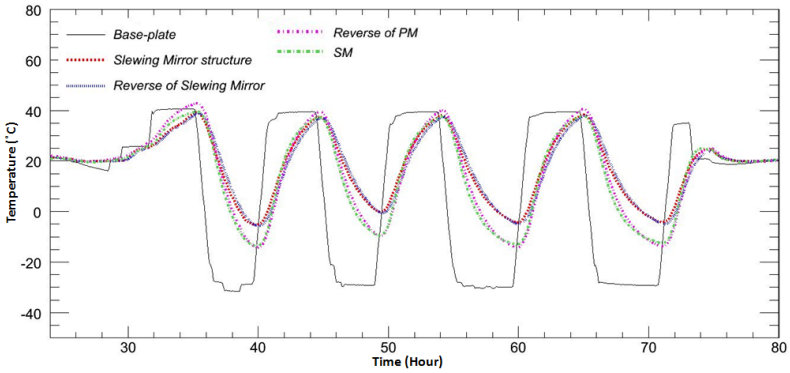

Fig. 13. Thermal response through thermocouples on PM, SM and slewing mirror.

The black solid line is the temperature variation at the base-plate receiving thermal loading directly. The red-dashed, blue-dotted lines are for the slewing mirror, magenta-dashed-dotted line from M1, and the green long dashed-dotted line from M2. We note that the responses of M1, M2 and the slewing mirror closely follow the base-plate temperature variation with some phase shifting and modulation. The resulting SMT thermal responses to the input heating and cooling profiles (i.e. ± 70 °C /hour) show the maximum 30 °C in temperature variation, where the temperature difference (i.e. thermal gradient) between M1 and M2 is less than the maximum ~5 °C, demonstrating good thermal conductivity across the SMT structure [22]. This results imply that, even if the base-plate is heated to increase the temperature by 56 °C over 48 min while orbiting over the day side of the Earth, the SMT structure would be subjected to only about 24 °C in average temperature increase. On the other hand, when it orbits around over the night side of the Earth, its temperature would decrease by only about –24 °C. Therefore the resulting thermal responses tend to confirm the analysis in Table 2 and the SMT optical performance stability during each orbital period. Detailed inspection after the thermal cycling revealed neither visible damages nor out-gassing signatures from the opto-mechanical structure, bond lines and mirror surfaces.

X, Y and Z axis vibration tests with input frequency sine sweep, random and shock patterns were performed. A total of 6 accelerometers were used, 4 attached to the SMT optics and the remaining 2 to the B axis motor and slewing mirror ring structure as shown in Fig. 14.

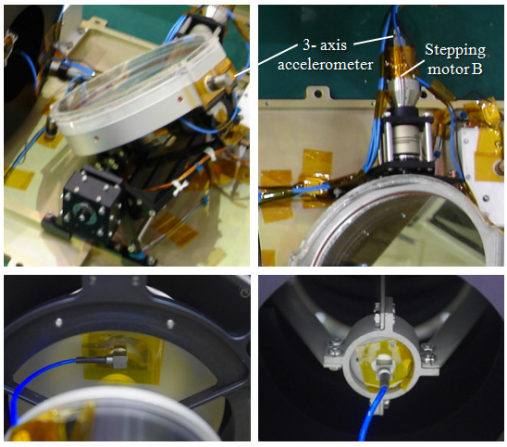

Fig. 14. Accelerometer placement on the SMT optics.

#179532 - $15.00 USD Received 8 Nov 2012; revised 27 Dec 2012; accepted 2 Jan 2013; published 23 Jan 2013

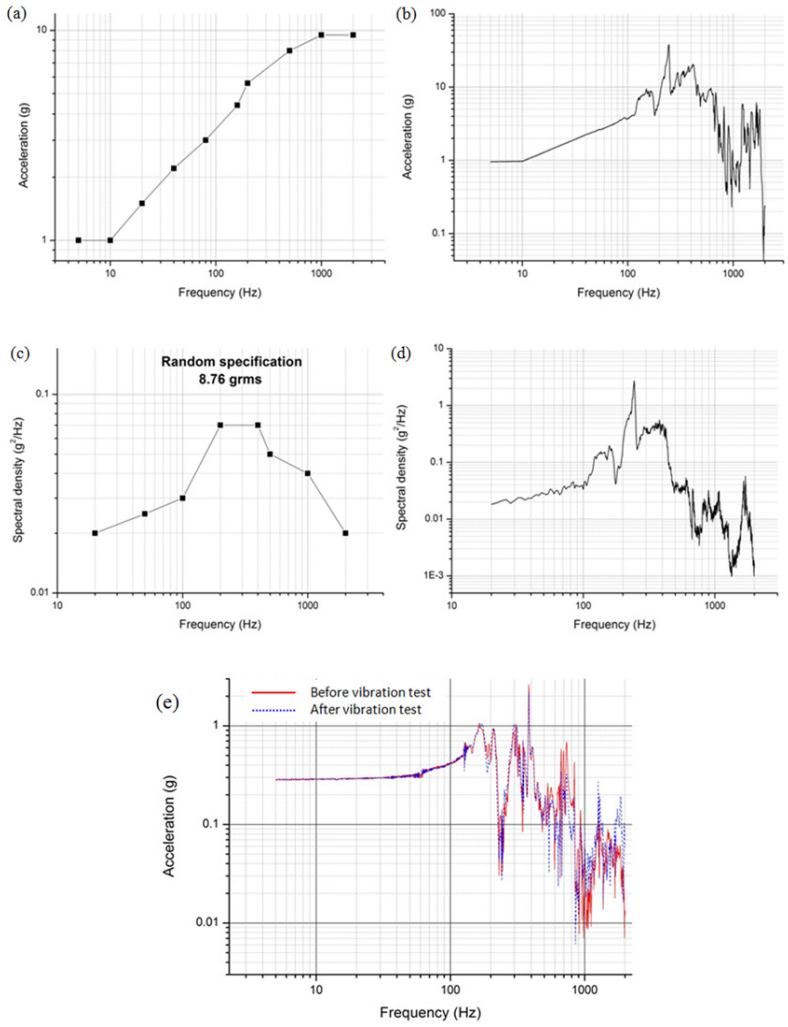

Fig. 15. Input conditions of (a) sine sweep and (c) random test, and example response from M2 accelerometer in (b) sine sweep, (d) random test, (e) low sine sweep test.

The sine sweep test input of up to 9.5 g from 5 to 2000 Hz, and the response results, are shown in Fig. 15(a). Figure 15(b) shows the maximum response of 38 g at 245 Hz. The instrument is designed to have a safety factor larger than 3 for 60 g load. The results prove that it is stiff enough to withstand the input stress. Figure 15(c) also shows the random frequency test inputs (8.76 g rms: RMS acceleration in units of gravity) and the M2 response along the launch direction as an example. As shown in Fig. 15(d), the response has the peak value at 244 Hz, which is similar to the 245 Hz peak from the sine sweep test. The low sine sweep test (0.3 g from 5 to 2000 Hz) was carried out before and after all other vibration tests. The resulting response after testing, in Fig. 15(e), is nearly identical to the "before" result, showing that the instrument retains its structural integrity.

#179532 - $15.00 USD Received 8 Nov 2012; revised 27 Dec 2012; accepted 2 Jan 2013; published 23 Jan 2013

3.2. Performance of SMT optics before and after space environment test

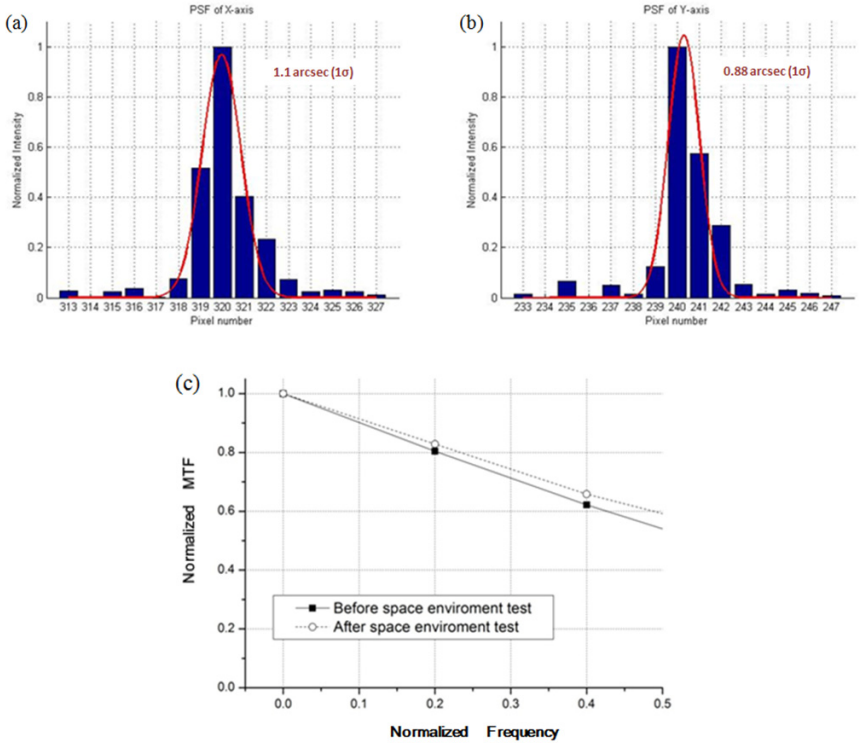

Fig. 16. Performance from measured PSF in X and –Y axis (a) and (b) after vibration test, and (c) derived MTF before and after space environment test.

The SMT MTF performances were estimated before and after the space environment test by using Point Spread Function (PSF) measurement. For simulated point source, we used parallel rays from a laser interferometer of 15.2 cm in aperture and a commercial CCD camera with 7.4 × 7.4 μm^2 pixel size was used to record the focused image of the incident light. The resulting PSF in X and Y-axis cuts are shown in Fig. 16(a) and Fig. 16(b). The bars are measured intensities and the solid line shows the best fit Gaussian function. The measurement of the PSFs after the test shows a 1σ width of 1.1 and 0.88 arcsec as seen in Fig. 16; in the "before" test the PSF widths were 1.04 and 0.94 arcsec (1σ) along the X and Y axes, respectively. The derived MTF data averaged over both axes are found to be 0.54 and 0.59 at the Nyquist frequency before and after the environment test. These results indicate that the SMT optics performance remains stable after the space environment test, demonstrating a robust survivability during launch and in-orbit operation.

4. System validation test of SMT optics

The flight model SMT including detector and readout electronics stands vertically for the system imaging test as appears in Fig. 17. The pre-flight model of RC telescope was used as a collimator, providing a parallel beam with ~4 arcsec in beam divergence.

#179532 - $15.00 USD Received 8 Nov 2012; revised 27 Dec 2012; accepted 2 Jan 2013; published 23 Jan 2013

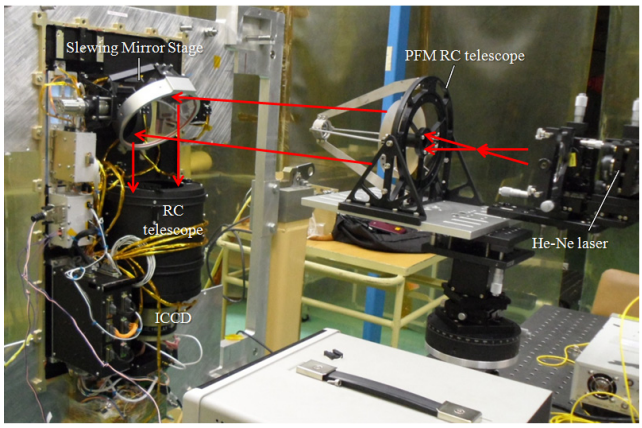

Fig. 17. Final SMT optics validation setup.

A He-Ne laser beam with 635 nm is focused on the PFM RC telescope focus point. It is then diverged before being collimated to a parallel beam to be fed to the slewing mirror that redirected it to M1. The beam is subsequently reflected by M2, and then focused onto the focal plane. To test pointing, we sent a trigger signal with a coordinate corresponding to a known source direction. The resulting focal images from before and after mirror slewing from one beam direction to another are shown in Fig. 18. The point is spread out 3 × 3 pixels on the focal plane, producing the SMT optics PSF shown in Fig. 19. The 4.3 arcsec (Y-slice, Gaussian fit 1σ) PSF is the result of the quadrature sum of the possible errors such as ~4 arcsec ICCD PSF, ~1 arcsec focal error due to gravity, and ~1 arcsec error from divergence of the parallel beam. It demonstrates that the constructed flight model SMT satisfies the angular resolution requirement.

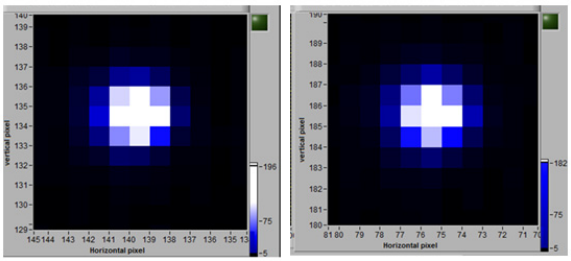

Fig. 18. The focal image size on the detector before and after mirror slewing.

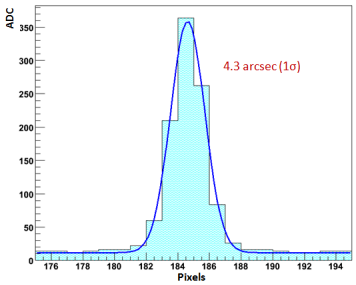

Fig. 19. Point spread function of flight model SMT.

#179532 - $15.00 USD Received 8 Nov 2012; revised 27 Dec 2012; accepted 2 Jan 2013; published 23 Jan 2013

5. Discussion

We are focused on two critical parameters of slewing mirror performance: slewing speed and pointing accuracy. The slewing speed of 1 second is fast enough for our needs. However the maximum rotation speed can be increased to achieve rotation times of just hundreds of ms, but at the expense of larger power consumption and longer settling time. The pointing accuracy is first determined by the finite teeth spacing of the drive gearing, also called "backlash". Smaller or finer backlash improves the pointing accuracy. We have chosen gears that satisfy our experimental requirement, 2.56 arcmin of accuracy, a value that is much smaller than SMT's FOV (17 arcmin).

For larger mirrors, the moment of inertia must be taken into account because it affects the pointing stability of satellite itself. In our case, the ratio of slewing mirror mass and moment of inertia to that of the spacecraft is negligible, and thus the torques from our motors produce negligible changes in satellite orientation. However, for a larger mirror, this may not be the case and some kind of counter-rotating mechanism may be required to keep the spacecraft pointing stable during rotation. Consider the moment of inertia of a uniform density disk-shaped mirror of radius r and thickness d, i.e. $I = 1/4Mr^2 + 1/12Md^2$. Typically the aspect ratio of such mirrors is around 1/8 [22]. Therefore, taking the uniformly increasing the disk ($d \sim r$, $M \sim r^3$), we find that $I \sim r^5$. The damping amplitude is proportional to $\exp[-t/t_0]$, where t_0 is proportional to I, thus the time constant (i.e. settling time) is also proportional to r^5. Now one can reduce the mass (M) and thickness (d) substantially, otherwise it would be extremely expensive to use such mirrors in space. We reduced our mirror mass by 57% over the ~1.3 kg typical mass, though we could have made the reduction up to 80% with much higher cost.

For a future UFFO space mission with a 40 cm aperture SMT, there will be technical challenges as discussed in above. Further reduction of mass, in principle up to 80%, typically 60~70%, would be available with careful design and precision lightweight technology. Figure 20 shows the relation of slewing mirror mass (hence moment of inertia) versus SMT aperture size, where 70% mass reduction and 1/8 of aspect ratio are assumed. The 40 cm aperture SMT requires a mass of ~7.5 kg that could be accommodated on small spacecraft.

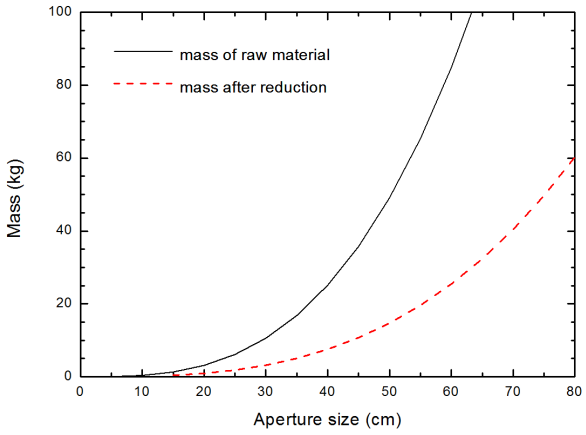

Fig. 20. SMT aperture size versus mass, assuming the 70% lightweight and aspect ratio of 1/8.

6. Conclusion

To enable for the first time systematic exploration of UV/optical GRB light curves earlier than 60 s after the gamma ray trigger, the UFFO missions have been proposed by utilizing a novel SMT concept with a fast slewing mirror. The SMT of 10 cm in aperture size has been designed, constructed and its flight instrument is now integrated in the *Lomonosov* satellite pending launch in 2013. Uniquely, SMT uses a fast steering mirror, instead of controlling the attitude of a whole satellite or telescope body, to point and track the target GRB. This paper

#179532 - $15.00 USD Received 8 Nov 2012; revised 27 Dec 2012; accepted 2 Jan 2013; published 23 Jan 2013

described the design, construction and laboratory performance tests that prove its capability of measuring the early light curves. We note that the SMT provides a ~4.3 arcsec (1σ width) PSF over 17 × 17 arcmin^2 in IFOV. And the angular resolution will be recovered up to 0.5 arcsec after the centroiding algorithm. This stationary FOV can be expanded to cover ± 35 degrees in operational FOV within about 1 s after the trigger. The initial laboratory measurements show that it would take about 1.5~1.8 s to slew over this field with the current non-optimized motor control algorithm. However, we remain confident that the slew time can be reduced to less than 1 s when controlled by the optimized motor control software that will be implemented before the instrument launch. The UFFO SMT is will be the very first space instrument using a fast slewing mirror for in-orbit observation of the GRB UV/optical emission, promising breakthroughs in understanding GRB physics, one of the most interesting astrophysics research fields in the 21st century.

Acknowledgments

This research was supported by the Korean Creative Research Initiatives (RCMST) of MEST/NRF, the Basic Science Research program of MEST/NRF (2010-0025056), the World Class University program of MEST/NRF (R32-2009-000-10130-0), the Spanish MINECO project AYA-2009-14027-C05-01, AYA-2011-29936-C05-01, AYA-2012-39727-C03-01, and AYA 2009-14000-C03-01/ESP, Taiwan's National Science Council Vanguard Program (100-2119-M-002-025) LeCosPA of National Taiwan University, Program of development of Lomonosov Moscow State University and Korean programs NRF 2012-0006632, 2010-0029390 and Yonsei-KASI joint research for the Frontiers of Astronomy and Space Science Program 2012. We thank Samsung Electronics (Super-precision Optics Lab., Imaging Division) for production of SMT mirrors, the National Space Organization (NSPO) of Taiwan and Nauchno-issledovatelskij institut elektromehaniki (NIIEM) of Russia for instrument space qualification, SCHOTT KOREA for consulting on the design of a light-weight mirror, and Dr. Yang of KRISS and H. K. Lee of Samsung for valuable discussions.

#179532 - $15.00 USD Received 8 Nov 2012; revised 27 Dec 2012; accepted 2 Jan 2013; published 23 Jan 2013